Journal of ELECTRONIC MATERIALS, Vol. 42, No. 1, 2013
DOI: 10.1007/s11664-012-2272-6

Preparation, Characterization, and Microwave Dielectric Properties of $Sr_2La_3Nb_{1-x}Ta_xTi_4O_{17}$ ($0 \le x \le 1$) Ceramics

ABDUL MANAN,[1,3] IBRAHIM QAZI,[2] and ATTA ULLAH[1]

1.—Department of Physics, University of Science and Technology, Bannu 28100, KPK, Pakistan. 2.—Department of Materials Science and Engineering, Institute of Space Technology, Islamabad 44000, Pakistan. 3.—e-mail: Abdul_Manan_sher@yahoo.com

$Sr_2La_3Nb_{1-x}Ta_xTi_4O_{17}$ ($0 \le x \le 1$) ceramics were processed via a solid-state mixed oxide route. $Sr_2La_3Nb_{1-x}Ta_xTi_4O_{17}$ ($0 \le x \le 1$) solid solutions were single phase in the whole range of x values within the x-ray diffraction (XRD) detection limit. The microstructure comprised elongated and needle-shaped grains. The ceramics exhibit relative permittivity (ε_r) of 73 to 68.6, product of unloaded quality factor and resonant frequency (Q_uf_0) of 7100 GHz to 9500 GHz, and temperature coefficient of resonant frequency (τ_f) of 78.6 ppm/°C to 56.6 ppm/°C.

Key words: SEM, microwave, materials, ceramics

INTRODUCTION

Recent technological developments in wireless telecommunication systems utilizing microwave dielectric ceramics as resonators, filters, and other components have increased interest in designing and engineering new materials for better performance and miniaturization of microwave components. Materials for commercial applications as dielectric resonators (DRs) require high relative permittivity ($\varepsilon_r > 24$), near-zero temperature coefficient of resonant frequency ($\tau_f \approx 0$ ppm/°C), and a high unloaded quality factor Q_u, generally reported as a product with the frequency f_0 at which it is measured ($Q_uf_0 \approx 30{,}000$ GHz). For certain applications, e.g., antennas, the values of τ_f and Q_uf_0 can be compromised to ±10 ppm/°C and >10,000 GHz, respectively; however, ε_r must be high, as this leads to a reduction in device size. Several materials have been employed as DRs in mobile phone handsets and base stations, but the search for materials with ultralow losses (high Q_uf_0), $\tau_f \approx 0$, and $\varepsilon_r > 50$[1–3] continues.

Dielectric ceramics with general formula $A_nB_nO_{3n+2}$ have been investigated for practical applications as DRs exhibiting high ε_r; e.g., Jawahar et al.[4] found the microwave dielectric properties of $CaLa_4Ti_5O_{17}$ ceramics sintered at 1625°C to be $\varepsilon_r \approx 53$, $\tau_f \approx -20$ ppm/°C, and $Q_uf_0 \approx 17{,}359$ GHz. The microwave dielectric properties of $CaLa_4Ti_5O_{17}$ ceramics were improved by substituting Ca^{2+} ions for Zn^{2+} ions.[5] Addition of 0.5 wt.% CuO to $Ca_{0.99}Zn_{0.01}La_4Ti_5O_{17}$ ceramics resulted in $\varepsilon_r \approx 57$, $Q_uf_0 \approx 15{,}000$ GHz, and $\tau_f \approx -8.16$ ppm/°C after sintering at 1450°C for 4 h.[6] Recently, Manan et al.[7] investigated the dielectric properties of $Sr_{5-x}Ca_xNb_4TiO_{17}$ ($x = 0$ to 5) ceramics, and $Sr_2Ca_3Nb_4TiO_{17}$ was reported to exhibit good properties with $\varepsilon_r \approx 53$ and $\tau_f \approx -6.5$ ppm/°C, although Q_uf_0 (~1166 GHz) was too low. More recently, the authors have investigated the microwave dielectric properties of $SrLa_4Ti_5O_{17}$ in the $Sr_{5-x}La_xNb_{4-x}Ti_{1+x}O_{17}$ ($x = 4$) series and reported $\varepsilon_r \approx 60.8$, $Q_uf_0 \approx 9969$ GHz, and $\tau_f \approx 117$ ppm/°C.[8,9] The high positive τ_f precluded its use as a DR. τ_f of $SrLa_4Ti_5O_{17}$ was tuned to zero by suitable dopants at the A-site of the perovskite structure but at the cost of decreasing ε_r and Q_uf_0 value.[10] However, to get materials with $\varepsilon_r > 50$, $Q_uf_0 >$ 10,000 GHz, and near-zero τ_f, the microwave dielectric properties of some new $Sr_2La_3Nb_{1-x}Ta_xTi_4O_{17}$ ($0 \le x \le 1$) ceramics were investigated in this work.

EXPERIMENTAL PROCEDURES

$Sr_2La_3Nb_{1-x}Ta_xTi_4O_{17}$ ($0 \le x \le 1$) ceramics were fabricated using a solid-state mixed oxide route.

(Received March 27, 2012; accepted September 15, 2012; published online October 17, 2012)

$SrCO_3$ (Aldrich, 99+%) and $CaCO_3$ (Aldrich, 99+%) were dried at ~185°C, while La_2O_3 (Aldrich, 99.95%), Nb_2O_5 (Aldrich, 99.95%), Ta_2O_5 (Aldrich, 99.95%), and TiO_2 (Anatase, Aldrich, 99+%) were dried at 900°C for 5 h to remove the moisture prior to weighing in order to ensure the correct initial stoichiometry of the compounds. The dried carbonates and oxides were weighed in stoichiometric ratios and wet ball-milled for 24 h in a disposable polyethylene mill jar, using Y-toughened ZrO_2 balls as grinding medium and 2-isopropanol as lubricant to make freely flowing slurries. The slurries were dried in an oven kept at ~95°C. The resulting powders were sieved and calcined in air at 1350°C for 6 h at heating/cooling rate of 5°C/min. The calcined powders were ground in a mortar and pestle for ~45 min to make fine powders. The powders were pressed into 4-mm- to 5-mm-high and 10-mm-diameter pellets at 80 MPa. The green bodies were placed on a platinum foil and sintered in air from 1450°C to 1600°C for 4 h at heating/cooling rates of 5°C/min. Phase analysis of sintered crushed pellets was carried out using a Philips x-ray diffractometer operating at 30 kV and 40 mA at scan rate of 1°/min from $2\theta = 10°$ to 70° at step size of 0.02°. A STOE PSD x-ray diffractometer with Cu K_α radiation (λ = 1.540598 Å) was used for the measurement of lattice parameters. Bulk densities of the sintered pellets were measured using the Archimedes method. The theoretical densities of the compounds were calculated using Eq. 1;

$$\rho_{th} = ZM/VA_g \quad (1)$$

where Z is the formula unit, M is the molecular weight, V is the volume of the unit cell, and A_g is the Avogadro number (6.022×10^{23} atoms/mole).

Dense sintered pellets were cut and finely polished before thermal etching for 30 min at temperatures ~10% less than their corresponding sintering temperatures, at heating/cooling rate of 5°C/min, for microstructural studies by scanning electron microscopy (SEM). The etched surfaces of the samples were gold-coated to avoid charging effect, and a JEOL 6400 SEM operating at 20 kV was used for microstructural examination.

Microwave dielectric properties were measured using an Agilent R3767CH network analyzer. The cylindrical pellets were placed on a low-loss quartz single crystal at the center of an Au-coated brass cavity, proposed by Krupka.[11] τ_f was measured by noting the temperature variation of the $TE_{01\delta}$ resonance in the temperature range of 20°C to 80°C using Eq. 2.

$$\tau_f = (f_2 - f_1)/f_1\Delta T, \quad (2)$$

where f_1 and f_2 are the resonant frequencies at 20°C and 80°C, respectively, and ΔT is the difference between the initial and final temperature.

RESULTS AND DISCUSSION

X-ray diffraction patterns recorded at room temperature from optimally sintered crushed and pulverized pellets of $Sr_2La_3Nb_{1-x}Ta_xTi_4O_{17}$ ($0 \le x \le 1$) ceramics are shown in Fig. 1. The reflections from all the compositions were identical and could be indexed according to the orthorhombic (*Pnnm*) $CaLa_4Ti_5O_{17}$ unit cell (PDF# 27-1059). There was no evidence of any second phase formation within the in-house x-ray diffraction (XRD) detection limits, which demonstrated the phase purity of all the sintered ceramics. The unit cell parameters were

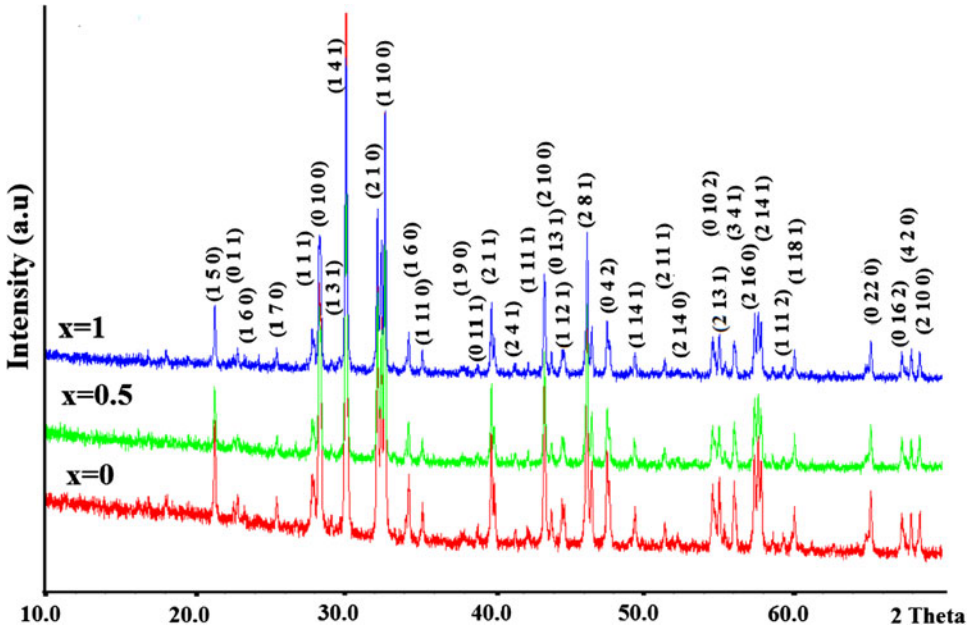

Fig. 1. XRD patterns from optimally sintered pulverized sample of $Sr_2La_3Nb_{1-x}Ta_xTi_4O_{17}$ ($0 \le x \le 1$) ceramics, showing single phase for each ceramics.

Table I. Preparation conditions, lattice parameters, relative densities, and microwave dielectric properties of $Sr_2La_3Nb_{1-x}Ta_xTi_4O_{17}$ ($0 \le x \le 1$) ceramics

Composition (x)	S.T. (°C)	a (Å)	b (Å)	c (Å)	ρ_r	ε_r	f_0 (GHz)	$Q_u f_0$ (GHz)	τ_f (ppm/°C)
0	1500	5.5595 (6)	31.526 (3)	3.9239 (5)	97.6	73	5.45	7100	78.6
0.5	1550	5.5624 (6)	31.528 (7)	3.9267 (4)	95.8	71.2	5.40	8400	67.3
1	1550	5.5632 (7)	31.532 (4)	3.9354 (6)	96.4	68.6	5.37	9500	56.6

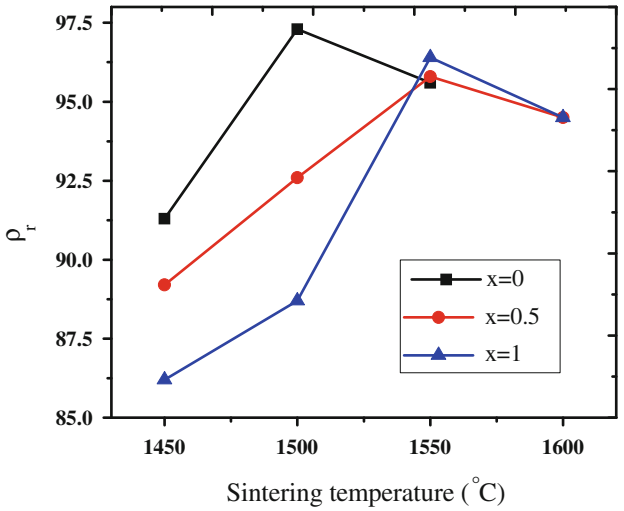

Fig. 2. Variation of ρ_r with sintering temperature for $Sr_2La_3Nb_{1-x}Ta_xTi_4O_{17}$ ($0 \le x \le 1$), showing $\rho_r > 95\%$ for each ceramic.

recalculated using the least-squares method from the XRD patterns of $Sr_2La_3Nb_{1-x}Ta_xTi_4O_{17}$ ($0 \le x \le 1$) ceramics and are compared in Table I. Although Nb^{5+} and Ta^{5+} ions are of almost equal size,[12] a small increase in the lattice parameters was observed for the Ta-doped compositions.

The variation of the relative density (ρ_r) of the $Sr_2La_3Nb_{1-x}Ta_xTi_4O_{17}$ ($0 \le x \le 1$) ceramics as a function of sintering temperature is shown in Fig. 2. Previous literature reveals that substitution of Ta^{5+} for Nb^{5+} increases the sintering temperature[13] also. In the present study, the sintering temperature was increased by ~50°C due to Ta^{5+} substitution for Nb^{5+}. All the ceramics were sintered to more than 95% of their theoretical density.

Secondary electron images (SEIs) from thermally etched gold-coated surfaces of $Sr_2La_3Nb_{1-x}Ta_xTi_4O_{17}$ ($0 \le x \le 1$) ceramics sintered at their optimum sintering temperatures are shown in Fig. 3. In general, the microstructures comprise densely packed ($\rho_r > 95\%$), elongated and needle-shaped grains—typical of layered perovskites with orthorhombic crystal structure,[14] although nonuniform grain growth could be seen in each sample, making the determination of exact grain size difficult; For example, elongated grains of >15 μm in length could be seen in the micrograph of the composition with $x = 0$.

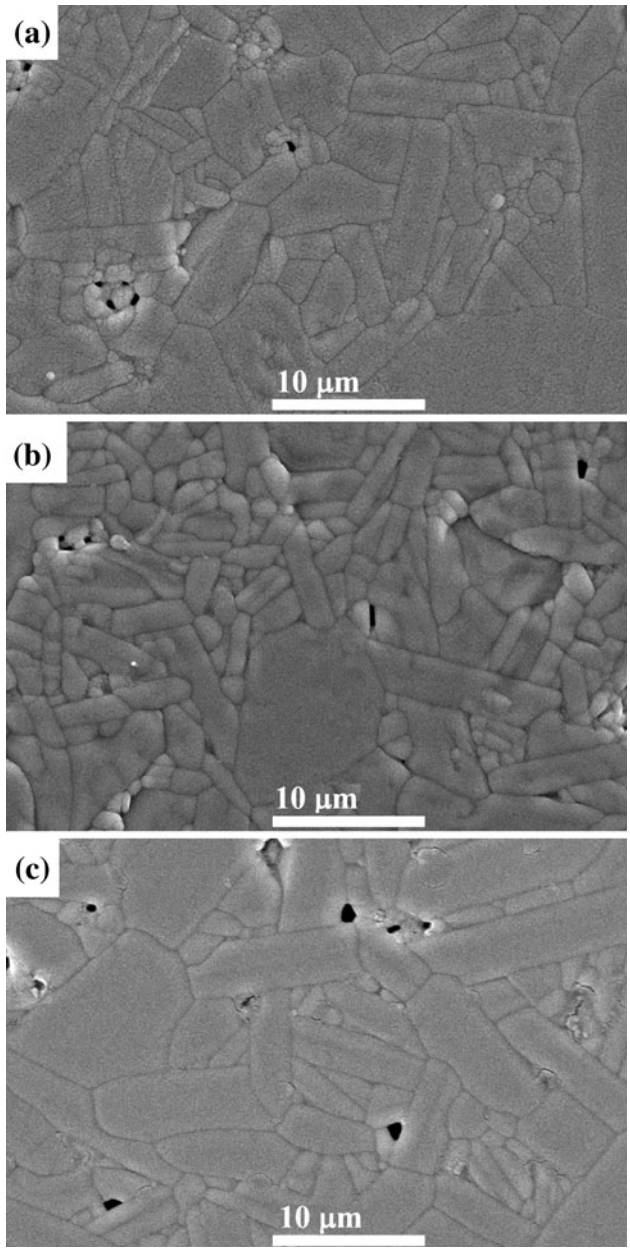

Fig. 3. SEIs of optimally sintered samples of $Sr_2La_3Nb_{1-x}Ta_xTi_4O_{17}$ ($0 \le x \le 1$) ceramics: (a) $x = 0$, (b) $x = 0.5$, and (c) $x = 1$, showing elongated and needle-shaped grain morphologies for each ceramic.

The variation of the microwave dielectric properties of $Sr_2La_3Nb_{1-x}Ta_xTi_4O_{17}$ ($0 \le x \le 1$) ceramics as a function of sintering temperature (from which the

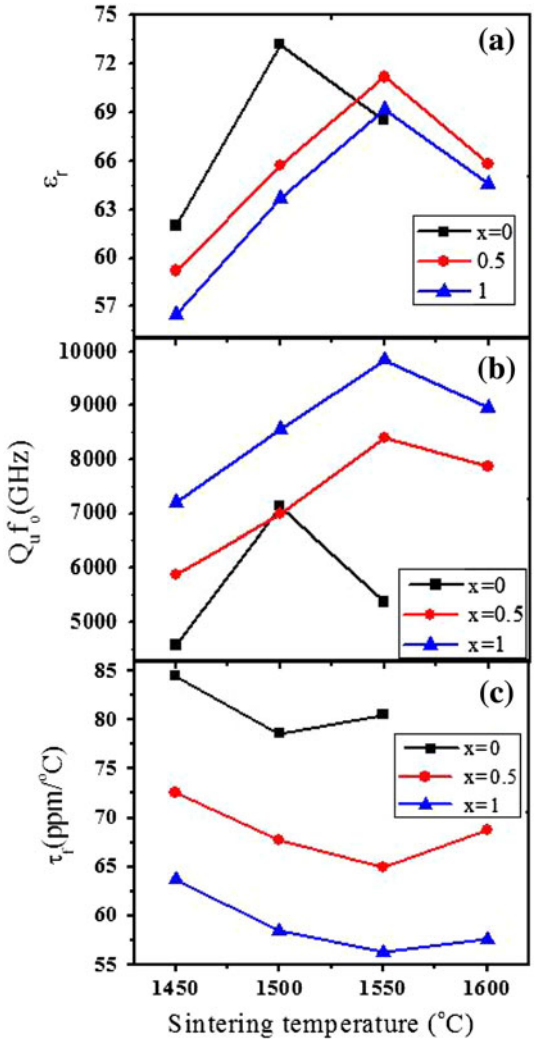

Fig. 4. Variation of (a) ε_r, (b) $Q_u f_0$, and (c) τ_f of $Sr_2La_3Nb_{1-x}Ta_xTi_4O_{17}$ ($0 \le x \le 1$) ceramics as a function of sintering temperature.

optimum sintering temperature could be obtained) is shown in Fig. 4. ε_r and $Q_u f_0$ exhibit similar behavior (Fig. 4a, b) to ρ_r with sintering temperature, while τ_f shows an opposite response (Fig. 4c). ε_r and $Q_u f_0$ for $x = 0$ are maximum at 1500°C; for $x = 0.5$ and 1, they are maximum at 1550°C due to their optimum higher densities at these sintering temperatures.

To better understand the effect of Ta content on the microwave dielectric properties, the well-sintered samples with relative density higher than 95% were selected so that the effects of density and microstructure could be neglected. The variation in the microwave dielectric properties for optimally sintered $Sr_2La_3Nb_{1-x}Ta_xTi_4O_{17}$ ($0 \le x \le 1$) ceramics as a function of Ta content are compared in Table I. τ_f decreases on substitution of Ta for Nb (Table I). These results are in accordance with previous literature, e.g., for $Ca_5Nb_{2-x}Ta_xTiO_{12}$ ($x = 0$ to 2)[15] and $Ba_4LaTiNb_{3-x}Ta_xO_{15}$.[16] Since the ionic polarizability of Ta^{5+} (4.73 Å^3) is larger than that of Nb^{5+} (3.93 Å^3),[17] ε_r should increase with increase in the Ta content, but in the present study ε_r decreased (Table I). This could be attributed to the larger short-range interaction parameter in O–Ta–O bond in comparison with O–Nb–O, which could also explain the increase in the $Q_u f_0$ value from 7100 GHz (at 5.45 GHz) to 9500 GHz (at 5.37 GHz) with increase in the Ta content from 0 to 1 as suggested by Ratheshes et al.[18] Reaney et al.[19] reported that the onset of structural phase transition is a major factor that influences the τ_ε value and established the relationship between the τ_ε value and the tolerance factor (τ) in complex perovskites. However, due to the same ionic radii and charge of Nb^{5+} and Ta^{5+}, the effect of the tolerance factor can be ignored in the present studies. Harrop[20] investigated the relationship between τ_c and ε_r. There is a linear relationship between ε_r and τ_c and therefore also between τ_f and ε_r. Therefore, τ_f decreased from 78 ppm/°C to 56.5 ppm/°C as the Ta content was increased from 0 to 1. Although Ta substitution for Nb leads to an increase in the $Q_u f_0$ value from 7100 GHz (at 5.45 GHz) to 9500 GHz (at 5.37 GHz) of the solid solution, a high $Q_u f_0$ value with τ_f close to 0 ppm/°C is required for possible microwave applications.

CONCLUSIONS

Single-phase, dense $Sr_2La_3Nb_{1-x}Ta_xTi_4O_{17}$ ($0 \le x \le 1$) ceramics were synthesized via a conventional solid-state sintering route. Optimum microwave dielectric properties, i.e., $\varepsilon_r \approx 68.6$, $Q_u f_0 \approx 9500$ GHz (5.37 GHz), and $\tau_f \approx 56.6$ ppm/°C, were achieved for $Sr_2La_3TaTi_4O_{17}$ ($x = 1$) ceramic. Further studies will be focused on improving the $Q_u f_0$ and controlling the τ_f values of $Sr_2La_3TaTi_4O_{17}$ ceramic for possible microwave applications.

ACKNOWLEDGEMENTS

The authors acknowledge financial support from the Higher Education Commission of Pakistan under the International Research Support Initiative Programme (IRSIP) and the electro-ceramics group in assisting the authors at the Electroceramics and Composite Laboratory, Department of Materials Science and Engineering, University of Sheffield, UK.

REFERENCES

1. L. Nedelcu, M.I. Toacsan, M.G. Banciu, and A. Loachim, *J. Alloys Compd.* 509, 477 (2011).
2. R. Freer and F. Azough, *J. Eur. Ceram. Soc.* 28, 1433 (2008).
3. I.M. Reaney and D. Idles, *J. Am. Ceram. Soc.* 89, 2068 (2006).
4. I.N. Jawahar, N. Santha, and M.T. Sebastian, *J. Mater. Res.* 17, 3084 (2002).
5. F. Zhao, Z. Yue, Z. Gui, and L. Li, *J. Am. Ceram. Soc.* 89, 3421 (2006).
6. Y.C. Chen and J.M. Tsai, *Jpn. J. Appl. Phys.* 47, 7959 (2008).
7. A. Manan, Y. Iqbal, and I. Qazi, *J. Mater. Sci.* 46, 3415 (2011).

8. A. Manan and Y. Iqbal, *J. Mater. Sci.: Mater. Electron.* 22, 1848 (2011).
9. Y. Iqbal, A. Manan, and I.M. Reaney, *Mater. Res. Bull.* 46, 1092 (2011).
10. A. Manan and Y. Iqbal, *Mater. Res. Bull.* 47, 883 (2012).
11. J. Krupka, K. Derzakowski, B. Riddle, and J.B. Jarvis, *Meas. Sci. Technol.* 9, 1751 (1998).
12. R.D. Shannan, *Acta. Cryst.* A32, 751 (1976).
13. L. Fang, C. Li, X. Peng, C. Hu, B. Wu, and H. Zhou, *J. Am. Ceram. Soc.* 93, 1229 (2010).
14. Y.C. Chen, S.L. Yao, R. Jie, and K.C. Chen, *J. Alloys Compd.* 486, 410 (2009).
15. P.V. Bijumon, P. Mohanan, and M.T. Sebastian, *Mater. Lett.* 57, 1380 (2003).
16. D. Gui, H. Zhang, L. Fang, and L. Xue, *J. Mater. Sci.: Mater. Electron.* 19, 543 (2008).
17. R.D. Shannon, *J. Appl. Phys.* 73, 348 (1993).
18. R. Ratheesh, M. Wohlecke, B. Berge, T. Wahlbrink, H. Haeuseler, E. Ruhi, R. Blachnik, P. Balan, N. Santha, and M.T. Sebastian, *J. Appl. Phys.* 88, 2813 (2000).
19. I.M. Reaney, E.L. Colla, and N. Setter, *Jpn. J. Appl. Phys.* 33, 3984 (1994).
20. P.J. Harrop, *J. Mater. Sci.* 4, 370 (1969).